International Journal of Mass Spectrometry 308 (2011) 126–132

Contents lists available at SciVerse ScienceDirect

International Journal of Mass Spectrometry

journal homepage: www.elsevier.com/locate/ijms

Gas-phase action spectroscopy of protoporphyrin IX (PP) and zinc-PP anions from 210 nm to 720 nm

Jean Ann Wyer*, Camilla Skinnerup Jensen, Steen Brøndsted Nielsen

Department of Physics and Astronomy, Aarhus University, Ny Munkegade 120, DK-8000 Aarhus C, Denmark

ARTICLE INFO

Article history:
Received 29 June 2011
Received in revised form 12 August 2011
Accepted 14 August 2011
Available online 22 August 2011

Keywords:
Protoporphyrin IX anions
Zinc–protoporphyrin IX anions
Action spectra
Absorption spectroscopy
Lifetime measurements

ABSTRACT

Action spectra of isolated gas-phase protoporphyrin IX (PP) and zinc-PP anions are presented here. Such spectra are valuable for protein biospectroscopy as absorption by proteins is often determined by the chromophores microenvironment which is often vacuum-like in the case of hydrophobic pockets. Ions were generated using electrospray ionisation, photoexcited in an electrostatic storage ring and their decay monitored in time. Action spectra were obtained by analyzing the time spectra at each wavelength.

1. Introduction

Porphyrins have been studied intensively as they are highly symmetric π-conjugated systems. These molecules are ubiquitous in nature and are responsible for key biological processes such as photosynthesis, oxygen transport and storage, and sensing [1–3]. One property of considerable interest is their electronic structure. However, this is strongly determined by the presence of a metal and its oxidation and spin state, axial ligands, peripheral substituents, and nearby water or amino acid residues. In general porphyrins and metalloporphyrins have an intense absorption band called the Soret band between 380 nm and 420 nm and two visible bands separated by ~1250 cm^{-1} between 500 nm and 600 nm denoted the *Q*-bands [4]. These bands are all due to $\pi\pi^*$ transitions [4]. The Soret band is the origin of the second excited singlet state, while in the *Q*-band region the lower-energy band is the electronic origin of the lowest-energy excited singlet state and the higher-energy band is a vibronic transition [4]. Furthermore, in the free-base, which has two hydrogens in the centre, there is a splitting of the bands in the visible region due to breaking of the D_{4h} symmetry of the porphyrin ring by the central proton axis (D_{2h} symmetry) [4].

Solvents affect the absorption by porphyrin molecules. Therefore, to elucidate the intrinsic electronic properties, gas-phase experiments are needed. Large amounts of work on evaporated porphyrin molecules have previously been published [4–8]. Protoporphyrin IX (PP) is of special interest as coordination of iron to it gives heme, which is found in the interior of hemoglobin and myoglobin proteins where it acts as a binding centre for dioxygen. However, as PP is difficult to vaporise, the only published work which deals with absorption by this important molecule is a recently published double-resonance spectroscopic study where the *neutral* molecules were vaporised using laser desorption [9]. In conventional methods, only porphyrin molecules with certain peripheral substituents can be brought into gas phase, and as band maxima positions are highly dependent on the substituents, such results fail to provide information on unmodified PP. Here, we provide action spectra of the protoporphyrin IX anion (PP^-) and the zinc(II)–protoporphyrin IX anion ($ZnPP^-$) isolated *in vacuo* (Fig. 1). Absorption band positions are compared with those of the following molecules and their zinc complex counterparts: octaethylporphyrin (OEP), porphin (P), etioporphyrin (Etio), tetrabenzoporphine (TBP), and tetraphenylporphyrin (TPP) (Fig. 1). Effects due to charge (electric field) and substituents are discussed.

Absorption spectra are generally measured by quantifying the loss of light after irradiation of a sample. Such light transmission experiments are often employed for measurements of neutral molecules in the gas phase, while for ions it is difficult to produce a vast enough number of ions. Here, action spectroscopy, which relies on the detection of fragmentation, was used to identify photon absorption.

2. Experimental

The experiments were performed at the electrostatic ion storage ring in Aarhus (ELISA) where keV ions circulate due to electrostatic sectors (see Fig. 2) [10,11]. Previous experiments using the same

* Corresponding author. Tel.: +45 8942 3601; fax: +45 8612 0740.
E-mail address: jeanwyer@phys.au.dk (J.A. Wyer).

1387-3806/$ – see front matter © 2011 Elsevier B.V. All rights reserved.
doi:10.1016/j.ijms.2011.08.015

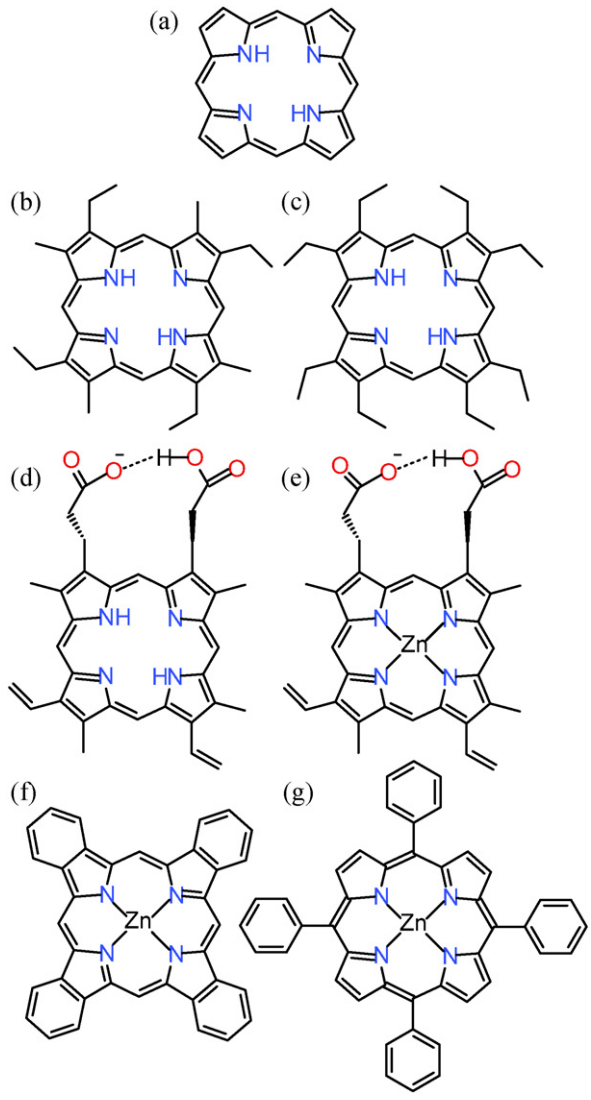

Fig. 1. (a) P, (b) Etio, (c) OEP, (d) PP^-, (e) $ZnPP^-$, (f) ZnTBP, and (g) ZnTPP.

method have previously been reported [12–15]. At each side of the ring there are two 10° electrostatic deflectors and one 160° deflector. Ions with the correct kinetic energy per charge are stored (22 keV/z). Electrospray ionisation was used to produce the deprotonated ions (even-electron species) which were subsequently accumulated in a 22-pole ion trap and thermally equilibrated by collisions with a helium buffer gas therein (room temperature). The ions were accelerated as an ion bunch to kinetic energies of 22 keV, and a bending magnet was used to select the appropriate ions. Following injection into the ring, the ions were stored for about 35 ms to ensure the decay of highly vibrationally excited ions before being irradiated by a nanosecond-long light pulse from a tunable laser (EKSPLA). This is an Nd:YAG (yttrium aluminum garnet) laser

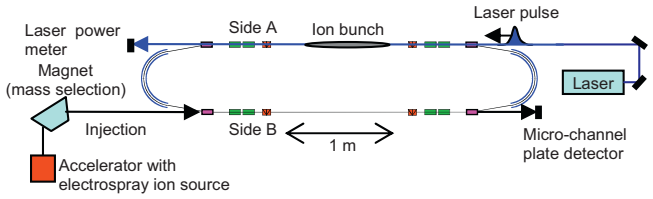

Fig. 2. Schematic of the ELectrostatic Ion Storage ring in Aarhus (ELISA). See text for details.

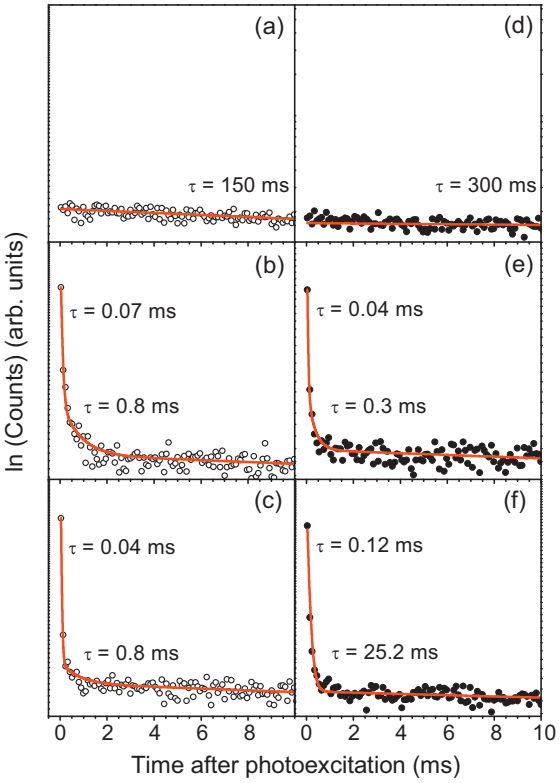

Fig. 3. Time spectra of PP^- (open circles) and $ZnPP^-$ (filled circles) ions after no photoexcitation, 400-nm photoexcitation and 580-nm photoexcitation ((a), (b), (c) and (d), (e), (f), respectively). The solid curves in (a) and (d) are exponential fits, while the remaining solid curves are fits of three exponentials to the data with one of the exponentials corresponding to the background decay. The laser pulse energies were (b) 0.3 mJ, (c) 5.9 mJ, (e) 0.05 mJ, and (f) 4.6 mJ.

where the third harmonic (355 nm) pumps an optical parametric oscillator [barium borate (BBO) crystal] which subsequently has a visible output. The length of the laser pulse is ~6 ns. To provide UV light the visible light was sent through a frequency-doubling crystal. The wavelength was scanned from 210 nm to 720 nm. The repetition rate of the experiment was 10 Hz. Dissociation resulted from both one- and two-photon absorption (*vide infra*). Lifetimes were obtained by monitoring the time dependence of the yield of neutrals hitting the microchannel plate (MCP) detector located at the end of the straight section (side B) opposite to the side where photoexcitation was performed (side A). A change in dissociation channel with excitation wavelength has little or no effect on our experiment since we sample all types of neutral fragments formed. Revolution times in the ring are 96 μs and 101 μs for PP^- and $ZnPP^-$. The pressure in the ring was of the order of 10^{-10} mbar, which set an upper limit of 1–2 s on the storage time. Compounds were purchased from Sigma–Aldrich and solutions were prepared by dissolving ZnPP in CH_2Cl_2/methanol (1:1) and PP in methanol.

3. Results and discussion

3.1. Time spectra

Time spectra after photoexcitation were measured by detecting the neutral fragments formed on one side of the ring (Fig. 3). These were produced ~48 μs and ~50 μs after photoexcitation for PP^- and $ZnPP^-$, respectively, in the first instance and then after successive rotations in the ring. In order to fit the data it was found that three separate exponentials were required. For PP^-, the fastest decays had time constants of the order of 10^{-2} ms, while the next

Table 1
Number of photons required to produce ions which decay with a rate associated with the short and long lifetimes.

	Soret	Q-band
PP^-		
Short lifetime	1	2
Long lifetime	1	1
$ZnPP^-$		
Short lifetime	2	1
Long lifetime	1	1[a]

[a] Deduced, see Section 3.

decays had time constants of the order of 10^{-1} ms. For $ZnPP^-$, the fastest decays had time constants of the order of 10^{-2} ms and 10^{-1} ms, while the next decays had time constants of the order of 10^{-1} ms and 10 ms, in the Soret and Q-band regions, respectively. After photon absorption, internal conversion from an electronically excited state back to the electronic ground state results in vibrationally excited ions, which dissociate into neutral and ionic fragments. Neutrals formed on the side of the ring opposite to where photoexcitation occurred were detected. We assume that vibrational cooling does not play a role since the timescales for emission of infrared light are normally longer than milliseconds. The two short lifetime components result from dissociation of the photoexcited ions. The time constant for the slowest decay in each case was set to that found after fitting the decay of ions when no photoexcitation occurred (CID decay). The values obtained were 150 ms for PP^- and 300 ms for $ZnPP^-$.

3.2. Dissociation energetics and photon dependences

For both PP^- and $ZnPP^-$, the dominant dissociation channel is loss of CO_2 which requires less than 1 eV [16]. Previous PM3 calculations show the ions possess about 1 eV of vibrational excitation energy assuming a temperature of 300 K [16]. Photoexcitation in the Q band region raises the internal energy by more than 2 eV. One photon is therefore enough to cause dissociation even in this low energy region, though entropic barriers likely slow down the dissociation [16].

In order to determine the number of photons that resulted in the measured dissociation, a study of the number of neutral photofragments as a function of laser pulse energy was undertaken (Table 1). For PP^- all absorption in the Soret band region is due to one photon absorption (see Fig. 4). Absorption in the Q-band region requires one-photon absorption to produce ions which decay with a rate associated with the longer timescale and appears to require between one and two photons to produce the ions which decay with a rate associated with the fastest timescale (see Fig. 5). Such a non-integer value is nonphysical and obtaining such a value is possibly due to incorrect fitting of the data; hence, a plot of the ratio of the number of photoexcited PP^- ions that decay with a rate associated with the smallest time constant to those that decay on the longer timescale was made in order to determine whether the two different sets of photoexcited ions are due to the absorption of a different number of photons. In such a plot it is easier to determine the dependence as a constant ratio implies absorption of the same number of photons, while a linear dependence through origin implies one absorbs one more photon than the other. In the present case, it can be seen that the ratio is clearly not constant. It seems as if there is a linear dependence between the two numbers up to about 4 mJ (see Fig. 6). The fact that the ratio is not constant implies that the photoexcited ions which decay with a rate associated with the fastest timescale have absorbed one more photon than those which decay with a rate associated with the longer timescale. The reason for the non-linear behaviour above 4 mJ is unclear. Values

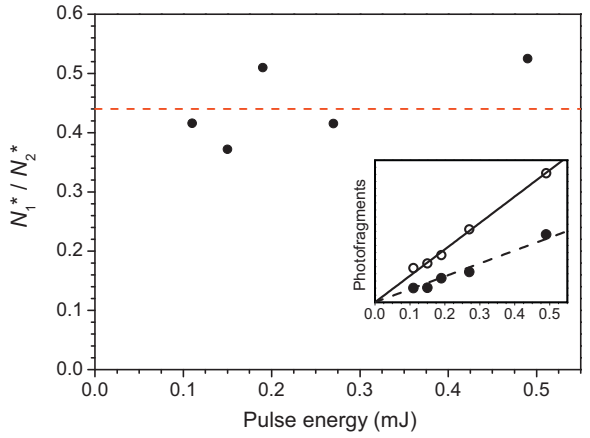

Fig. 4. Ratio of the number of photoexcited PP^- ions (380 nm) that decay with a rate associated with the smallest time constant (0.07 ms), N_1^*, to those that decay on a longer time period (0.8 ms), N_2^*, as a function of the laser pulse energy. The ratio is constant, as indicated by the red line. The inset shows the dependence of the number of photofragments from photoexcited ions that decay with a rate associated with the smallest time constant (filled circles) and those which decay on a longer time period (open circles) as functions of laser pulse energy. A linear fit for each data set is shown. (For interpretation of the references to color in this figure legend, the reader is referred to the web version of this article.)

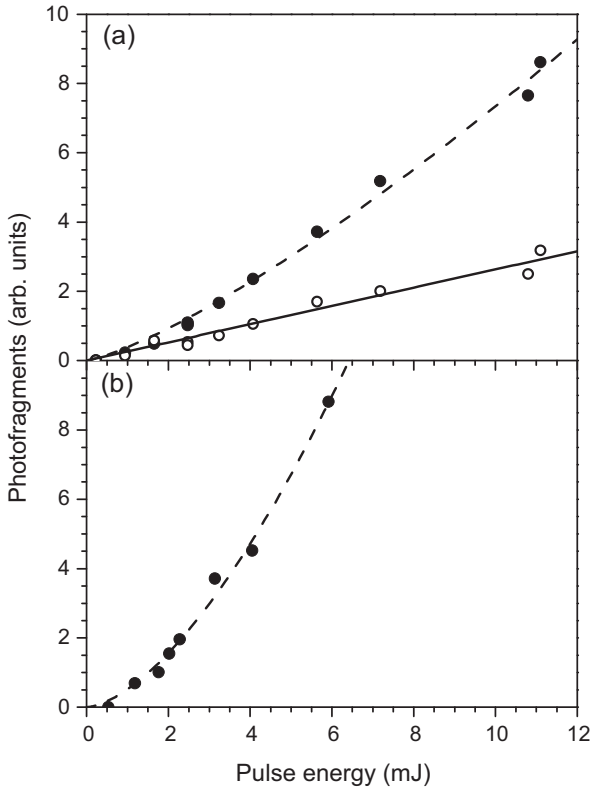

Fig. 5. (a) The dependence of the number of photofragments from photoexcited PP^- ions (500 nm) that decay with a rate associated with the smallest time constant (0.04 ms, filled circles) and those which decay on a longer time period (0.8 ms, open circles) as functions of laser pulse energy. A linear fit to the open circles (solid line) and a power-law fit to the closed circles (dashed curve), which gave a dependence to the pulse energy of power 1.3, are shown. (b) The dependence of the number of photofragments from photoexcited PP^- ions (580 nm) that decay with a rate associated with the smallest time constant (0.04 ms) as a function of laser pulse energy. A power-law fit to the data which gave a dependence to the pulse energy of power 1.6 is shown.

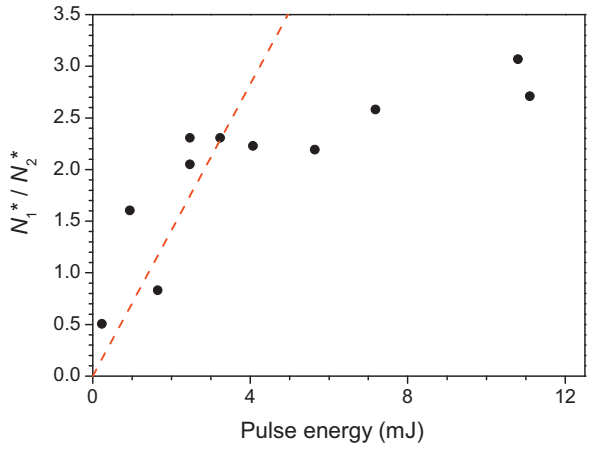

Fig. 6. Ratio of the number of photoexcited PP^- ions (500 nm) that decay with a rate associated with the smallest time constant (0.04 ms), N_1^*, to those that decay on a longer time period (0.8 ms), N_2^*, as a function of the laser pulse energy. The linear dependence up to about 4 mJ is indicated with a red line. (For interpretation of the references to color in this figure legend, the reader is referred to the web version of this article.)

for the time constants are in agreement with two-photon absorption in the *Q*-band region and one-photon absorption in the Soret band region as the short time constants in the higher wavelength *Q*-band region are lower than those in the Soret band region. Finally, it should be mentioned that significantly different cross sections for the absorption of the first and the second photon may result in the appearance of a one photon dependence. The second photon may be absorbed either by the electronically excited ions or hot ions formed after internal conversion, given that the length of the laser pulse is ~6 ns.

For $ZnPP^-$ it initially appeared as if it requires absorption of between one and two photons to produce ions which decay with a rate associated with the fastest timescale in the Soret band region (see Fig. 7). However, similar to the case above a plot of the ratio of the number of photoexcited $ZnPP^-$ ions that decay with a rate

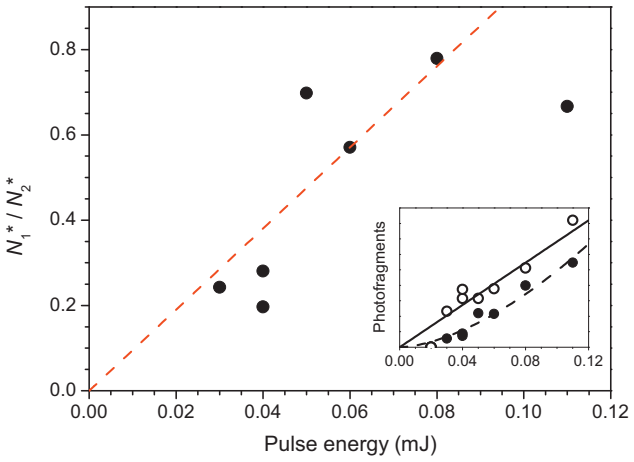

Fig. 7. Ratio of the number of photoexcited $ZnPP^-$ ions (407 nm) that decay with a rate associated with the smallest time constant (0.04 ms), N_1^*, to those that decay on a longer time period (0.3 ms), N_2^*, as a function of the laser pulse energy. The linear dependence up to 0.09 mJ is indicated with a red line. The inset shows the dependence of the number of photofragments from photoexcited ions that decay with a rate associated with the smallest time constant (filled circles) and those which decay on a longer time period (open circles) as functions of laser pulse energy. A linear fit to the open circles (solid line) and a power-law fit to the closed circles (dashed curve), which gave a dependence to the pulse energy of power 1.6, are shown. (For interpretation of the references to color in this figure legend, the reader is referred to the web version of this article.)

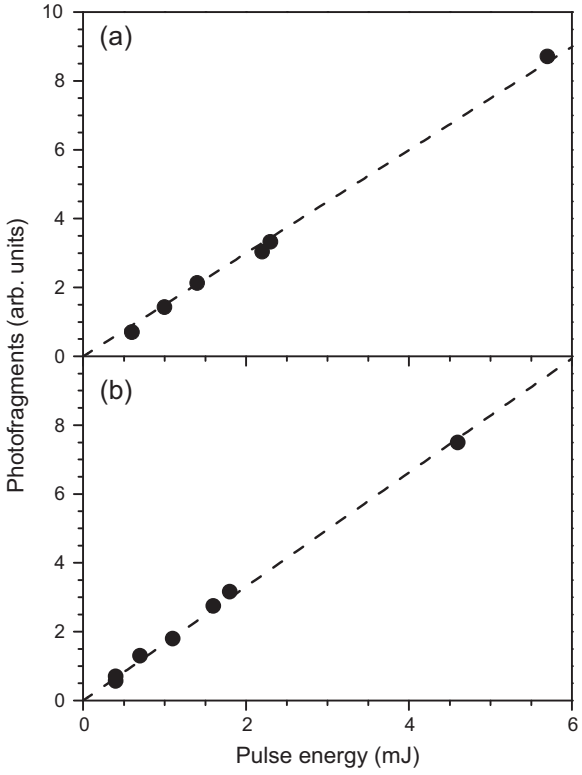

Fig. 8. The dependence of the number of photofragments from photoexcited $ZnPP^-$ ions ((a) 540 nm, (b) 575 nm) that decay with a rate associated with the smallest time constant (0.11 ms and 0.12 ms, respectively) as functions of laser pulse energy. Linear fits to the data are shown.

associated with the smallest time constant to those that decay on the longer timescale revealed the ratio is not constant and that there is possibly a linear dependence between the two numbers up to about 0.09 mJ. Hence, in this region it requires two photons to produce ions which decay with a rate associated with the fastest timescale and one photon for the ions which decay with the slower rate. In the *Q*-band region absorption is due to one photon absorption for the ions which decay on the shorter timescale (see Fig. 8). Note, the data quality is too low to make firm conclusions on the ions which decay on the longer timescale using the same method. However, if there was a two-photon dependence in the *Q*-band region, then the lifetime values in this region should be identical to those at half the wavelength where there is a one-photon dependence, e.g., $\tau_{600\,nm}$ should be equal to $\tau_{300\,nm}$. As this is not the case ($\tau_{600\,nm}$ = 27 ms and $\tau_{300\,nm}$ = 0.3 ms) it can be concluded that there is a one-photon dependence in the *Q*-band region.

The requirement of two time constants to describe photofragmentation could be a consequence of a number of factors. One such reason is the absorption of a different number of photons, as was seen for the absorption of *Q*-band light by PP^- ions. On the other hand, all dissociation after the absorption of Soret band light by PP^- ions was due to one-photon processes. It is possible that the longer time constant is due to intersystem crossing to a triplet state. A rate limiting spin flip is then required to reach the electronic ground state [14,16]. The triplet state lifetimes for PP free base in mulgofen, a nonionic surfactant of the poly(ethylene oxide) type, have been reported to be 3 ms [17], which is longer than our value of 0.8 ms in agreement with the fact that vibrational excitation increases the intersystem crossing rate. That triplet states play a role for the decay is supported by a recent pump–probe experiment on PP^- where photoexcited ions were seen to absorb red light [18]. In the case of $ZnPP^-$ multiple time constants in the *Q*-band region could be due to intersystem crossing to a triplet state or to the width of the

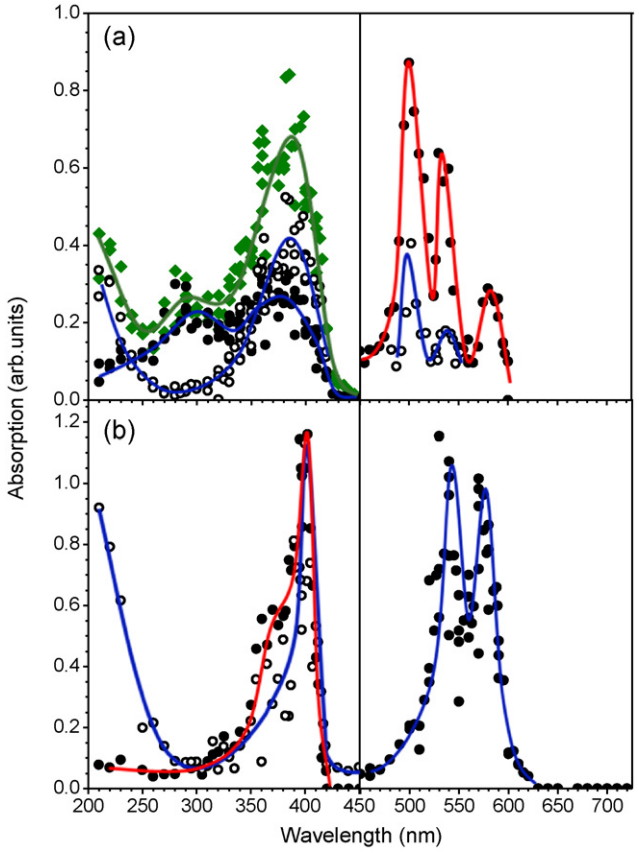

Fig. 9. Action spectra of (a) PP^- and (b) $ZnPP^-$ ions *in vacuo*. Spectra calculated from the short and long lifetime components are represented by closed and open circles. Curves were drawn to guide the eye, with the one- and two-photon action spectra represented by blue and red curves. The sum of short and long lifetime components for PP^- absorption in the Soret band is indicated in green. Data quality was too poor to calculate the long lifetime component spectrum for $ZnPP^-$ in the *Q*-band. A comparison of intensities of the Soret bands to those of *Q* bands is not valid from this experiment; the vertical line at 450 nm separates the two regions. (For interpretation of the references to color in this figure legend, the reader is referred to the web version of this article.)

internal energy distribution [19,20]. Each rate constant depends on the activation energy and preexponential factor for the dissociation process, and the internal energy. Here, however, two rate constants are sufficient to account for the decay.

3.3. Action spectra

Action spectra of (a) PP^- and (b) $ZnPP^-$ *in vacuo* are shown in Fig. 9. To obtain these spectra, three exponentials were first fitted to the time spectra for each wavelength; $y = A_1\exp(-t/\tau_1) + A_2\exp(-t/\tau_2) + A_3\exp(-t/\tau_3)$, where the first and second terms relate to the photoexcited ions which decay with time constants τ_1 and τ_2 (*vide supra*) and the last term accounts for CID decay. Fits were done under the constraint that time constants in each absorption band did not decrease with increasing λ. However, the action spectra look similar using free fits. From the fits, it was possible to calculate a number proportional to the total number of photoexcited ions, $N^*_{\mathrm{Ions},i} = A_i\tau_i$ (i is either 1 or 2). Finally, absorption cross sections were calculated using the following formula: $Abs_i = A_i\tau_i/(N_{\mathrm{Background}}(N_{\mathrm{Photons}})^x)$, where $N_{\mathrm{Background}}$ is the neutrals signal arising from CID prior to photoexcitation, which is proportional to the number of ions in the beam, and is included to account for variations in the ion beam intensity; N_{Photons} is the number of photons in the laser pulse; and x is either 1 or 2 for one- or two-photon absorption, respectively. Based on measurements on different days, we estimate the uncertainty in the relative absorption cross sections to be about 10%. A change in dissociation channel with excitation wavelength has little or no effect on our experiment since we sample all neutral fragments formed.

The action spectra (Fig. 9) are identical to absorption spectra under the assumptions that the fluorescence quantum yield is independent of excitation wavelength and that any prompt dissociation which occurs right after photoexcitation is being accounted for by the short time constant. The electron binding energies (*EBEs*) of PP^- and $ZnPP^-$ are not known but for comparison it is 3.4 eV for $CH_3CH_2COO^-$. A hydrogen bond between the carboxylate and the carboxylic acid is most likely present [14,21], which increases this value by ca. 0.4 eV (hydration free energy of $CH_3CO_2^-$) [21]. Finally, after considering the polarisability of the porphyrin ring, we take the *EBE* to be at least 3.8 eV, which implies that at wavelengths below ca. 326 nm the occurrence of some direct photodetachment cannot be excluded. As the detector is located on the other side of the ring to where photoexcitation occurs, no prompt processes are measured. Therefore, if electron photodetachment is occurring below ca. 326 nm, the neutrals from this process are not measured and the action spectra in this region may not represent absorption spectra.

For PP^- the short and long lifetime component spectra in the Soret band region are quite different. For the latter the band maximum is located at 386 nm. The sharp band seen at 355 nm is an artefact due to a different laser beam profile in a narrow region around 355 nm. A further band is observed at or below 210 nm. For the short lifetime component spectrum markedly different absorption is observed. There, little absorption is seen in the 210 nm region. Furthermore, a double band structure with maxima at 291 nm and 375 nm is observed. As mentioned above, it is possible that the long lifetime component is due to intersystem crossing to a triplet state. If that is indeed the case, then a comparison of the short and long lifetime components provides an indication of the triplet quantum yields as a function of wavelength. Total absorption in this region is indicated on the graph in green. In the *Q*-band, bands are located at 499 nm and 535 nm in both spectra, with a further band (581 nm) identified in the two-photon spectrum. Low data quality limits the long lifetime component spectrum range. The bands in both spectra are concurrent, which is in agreement with the fact that the power is relatively constant over this region, and with previous work by Kappes et al. [22] who found that for phthalocyanine the first and second photon had similar absorption cross sections.

For $ZnPP^-$, a sharp band is seen at 406 nm, while two prominent bands are seen at 550 nm and 594 nm. There are indications of a shoulder to the high-energy side of the Soret band in the one-photon spectrum; however, this is clearer in the two-photon spectrum.

As $ZnPP^-$ is a regular porphyrin, the metal orbitals have little effect on the absorption [4]. A comparison of our PP^- action spectrum to that of $ZnPP^-$ reveals that for PP^- the band below 210 nm appears to have blueshifted, the Soret band is broader and is blueshifted, and the bands in the *Q*-band differ. While we cannot measure below 210 nm and establish the exact maxima of the bands there, our results indicate that the band for $ZnPP^-$ is to the red of that for PP^-. It is well known that the Soret band is broader for free-base porphyrins than for metalloporphyrins [4]. A splitting of $\sim$1100 cm^{-1} is observed for the $ZnPP^-$ *Q*-band; this should be compared with a generally seen splitting of $\sim$1250 cm^{-1}. For a free-base porphyrin the *Q*-band splits ($\sim$3000 cm^{-1}) due to the asymmetry of the ring, and as each electronic excitation can couple to vibrations, there are a total of four bands in the visible region. Here, we observe a splitting due to asymmetry of $\sim$2800 cm^{-1}, while the vibronic transition associated with the higher energy band is located $\sim$1350 cm^{-1} away. Due to low statistics, we were unable

Table 2
Gas-phase absorption band maxima in nm.

	Soret	Q band			
	$B(0,0)$	$Q_y(1,0)$	$Q_y(0,0)$	$Q_x(1,0)$	$Q_x(0,0)$
P [6,8][a,d]	–	–	502.9	–	612.8
P [23][a,e]	372.5	483.5	511.5	575	627.5
OEP (neutral) [24][b,f]	384	495	529	582	635
PP (neutral) [9][b,g]	–	496	525	581	629
PP anion[c,h]	386 ± 3	499 ± 3	535 ± 3	581 ± 3	–
	Soret	Q band			
	$B(0,0)$	$Q(1,0)$	$Q(0,0)$		
Zn-Etio [24][a,i]	388	535.5	571		
Zn-OEP [4,24][a,j]	388.5	535	572		
Zn-TBP [7][a,k]	390.2	–	603.2		
Zn-TPP [23][a,l]	406	550	594		
Zn-PP anion[c,m]	401 ± 3	542 ± 3	576 ± 3		

Temperatures for the measurements were as follows (temperatures separated by a comma indicate the temperatures for the Soret band and Q-band, respectively).
[a] From tabulated data/from paper text.
[b] Estimated from graph.
[c] Current data.
[d] Ultracold.
[e] 393 °C, 322 °C.
[f] 295 °C, 387 °C.
[g] Cold.
[h] Room temperature.
[i] 355 °C, 400 °C.
[j] 346 °C, 379 °C.
[k] Ultracold.
[l] 393 °C, 445 °C.
[m] Room temperature.

to measure the fourth Q-band; however, our results suggest it is located at ~630 nm (assuming a vibronic splitting of 1350 cm^{-1}).

In order to assess the effect the charge has on the absorption bands of PP we compare our results to the very recent results for the PP neutral molecule [9], for which the subsituents are the same and only the charge differs. The absorption band maxima for this molecule and several others within the porphyrin family are listed in Table 2. There it can been seen that the $Q_y(0,0)$ and $Q_y(1,0)$ band maxima for the neutral PP molecule are blue-shifted from those of the anion. This shift is either due to the higher temperature in our experiment or due to the anion having an excited state which is more polarisable than the ground state allowing for a better organization of the π-electron cloud in the excited state than in the ground state. It is not clear why the $Q_x(1,0)$ maxima are in agreement. Upon consideration of the other molecules listed in Table 2, it is seen that the addition of substituents to the ring causes a redshift. Furthermore, the maxima of PP^- are slightly redshifted from those of OEP. This is likely due to the higher π-conjugation provided by the vinyl groups, though the charge may also play a role.

For the Zn–porphyrins, it is seen that the bands in both the visible and the UV regions are comparable for Zn-Etio and Zn-OEP due to the similarities between the molecules. Our present work has shown that the bands for $ZnPP^-$ are located to the red of those for the aforementioned molecules, possibly due to increased π-conjugation. Finally, while the molecules ZnTBP and ZnTPP are markedly different to the other molecules and a clear comparison is hence challenging, their absorption maxima have been included for completeness.

4. Conclusion

Absorption bands were measured at 299 nm, 386 nm, 499 nm, 535 nm and 581 nm for PP^- and at 401 nm, 542 nm and 576 nm for $ZnPP^-$. This is the first time the absorption by these ions has been probed. A comparison with previously measured molecules was made in order to assess the impact of substituents and charge state on the absorption profile. Peripheral substituents cause a redshift of all bands, particularly when conjugation is increased. It is difficult to extricate the effect due to charge from that due to substituents and temperature; a fact which should be considered an incentive for undertaking high level theoretical calculations to facilitate a deeper understanding of the effects of charge on porphyrins.

Acknowledgement

Support from Lundbeckfonden is gratefully acknowledged.

References

[1] J.M. Berg, J.L. Tymoczko, L. Stryer, Biochemistry, 6th ed., W.H. Freeman and Company, New York, 2007.
[2] M.W. Makinen, A.K. Churg, Structural and analytical aspects of the electronic spectra of heme proteins, in: A.B.P. Lever, H.B. Gray (Eds.), Iron Porphyrins, Part 1, Addison-Wesley Publishing Company, Inc., Reading, MA, 1983.
[3] K. Kalyanasundaram, Photochemistry of Polypyridine and Porphyrin Complexes, Academic Press, London, 1997.
[4] M. Gouterman, Optical spectra and electronic structure of porphyrins and related rings, in: D. Dolphin (Ed.), The Porphyrins, Volume III, Physical Chemistry, Part A, Academic Press, 1978.
[5] M. Gouterman, J. Mol. Spectrosc. 6 (1961) 138–163.
[6] U. Even, J. Magen, J. Jortner, Chem. Phys. Lett. 88 (1982) 131–134.
[7] U. Even, J. Jortner, J. Friedman, J. Phys. Chem. 86 (1982) 2273–2276.
[8] U. Even, J. Jortner, Z. Berkovitchyellin, Can. J. Chem.-Rev. Can. Chim. 63 (1985) 2073–2080.
[9] J.M. Beames, A.J. Hudson, T.D. Vaden, J.P. Simons, Phys. Chem. Chem. Phys. 12 (2010) 14076–14081.
[10] S.P. Møller, Nucl. Instrum. Meth. Phys. Res. A 394 (1997) 281–286.
[11] J.U. Andersen, P. Hvelplund, S. Brøndsted Nielsen, S. Tomita, H. Wahlgreen, S.P. Møller, U.V. Pedersen, J.S. Forster, T.J.D. Jørgensen, Rev. Sci. Instrum. 73 (2002) 1284–1287.
[12] J.A. Wyer, A. Ehlerding, H. Zettergren, M.-B.S. Kirketerp, S. Brøndsted Nielsen, J. Phys. Chem. A 113 (2009) 9277–9285.
[13] M.K. Lykkegaard, A. Ehlerding, P. Hvelplund, U. Kadhane, M.-B.S. Kirketerp, S. Brøndsted Nielsen, S. Panja, J.A. Wyer, H. Zettergren, J. Am. Chem. Soc. 130 (2008) 11856–11857.
[14] M.K. Lykkegaard, H. Zettergren, M.-B.S. Kirketerp, A. Ehlerding, J.A. Wyer, U. Kadhane, S. Brøndsted Nielsen, J. Phys. Chem. A 113 (2009) 1440–1444.
[15] J.A. Wyer, S. Brøndsted Nielsen, J. Chem. Phys. 133 (2010) 084306.

[16] M.R. Calvo, J.U. Andersen, P. Hvelplund, S. Brøndsted Nielsen, U.V. Pedersen, J. Rangama, S. Tomita, J.S. Forster, J. Chem. Phys. 120 (2004) 5067–5072.
[17] R.S. Sinclair, D. Tait, T.G. Truscott, J. Chem. Soc., Faraday Trans. I 76 (1980) 417–425.
[18] K. Støchkel, J.A. Wyer, M.B.S. Kirketerp, S. Brøndsted Nielsen, J. Am. Soc. Mass Spectrom. 21 (2010) 1884–1888.
[19] J.U. Andersen, H. Cederquist, J.S. Forster, B.A. Huber, P. Hvelplund, J. Jensen, B. Liu, B. Manil, L. Maunoury, S. Brøndsted Nielsen, U.V. Pedersen, J. Rangama, H.T. Schmidt, S. Tomita, H. Zettergren, Phys. Chem. Chem. Phys. 6 (2004) 2676–2681.
[20] J.U. Andersen, H. Cederquist, J.S. Forster, B.A. Huber, P. Hvelplund, J. Jensen, B. Liu, B. Manil, L. Maunoury, S. Brøndsted Nielsen, U.V. Pedersen, H.T. Schmidt, S. Tomita, H. Zettergren, Eur. Phys. J. D 25 (2003) 139–148.
[21] A.T. Blades, J.S. Klassen, P. Kebarle, J. Am. Chem. Soc. 117 (1995) 10563–10571.
[22] M. Kordel, D. Schooss, S. Gilb, M.N. Blom, O. Hampe, M.M. Kappes, J. Phys. Chem. A 108 (2004) 4830–4837.
[23] L. Edwards, D.H. Dolphin, M. Gouterman, A.D. Adler, J. Mol. Spectrosc. 38 (1971) 16–32.
[24] L. Edwards, D.H. Dolphin, M. Gouterman, J. Mol. Spectrosc. 35 (1970) 90–109.